

Quantum Numbers of Recently Discovered Ω_c^0 Baryons from Lattice QCD

M. Padmanath^{1,*} and Nilmani Mathur^{2,†}

¹*Institut für Theoretische Physik, Universität Regensburg,
Universitätsstrasse 31, 93053 Regensburg, Germany.*

²*Department of Theoretical Physics, Tata Institute of Fundamental Research,
Homi Bhabha Road, Mumbai 400005, India.*

We present the ground and excited state spectra of Ω_c^0 baryons with spin up to 7/2 from lattice quantum chromodynamics with dynamical quark fields. Based on our lattice results, we predict the quantum numbers of five Ω_c^0 baryons, which have recently been observed by the LHCb Collaboration. Our results strongly indicate that the observed states $\Omega_c(3000)^0$ and $\Omega_c(3050)^0$ have spin-parity $J^P = 1/2^-$, the states $\Omega_c(3066)^0$ and $\Omega_c(3090)^0$ have $J^P = 3/2^-$, whereas $\Omega_c(3119)^0$ is possibly a $5/2^-$ state.

PACS numbers: 12.38.Gc, 12.38.-t, 14.20.Lq

The study of heavy hadrons is passing through an incredible era with the discovery of numerous heavy subatomic particles [1]. As a result, there has been significant resurgence in scientific interest to explore the spectrum of strongly interacting heavy hadrons. To add to this proliferated interest in hadron spectroscopy, the LHCb Collaboration has recently reported its unambiguous observation of five new resonances in $\Xi_c^+ K^-$ invariant mass distribution based on pp collision data in the energy range between 3000 and 3120 MeV [2]. These resonances have been interpreted as the excited states of Ω_c^0 baryon. While the masses and widths of these resonances are known precisely, their other important quantum numbers (J^P), namely, spin (J) and parity (P), are yet unknown. In this Letter, we predict the quantum numbers of these five Ω_c^0 resonances using lattice quantum chromodynamics (lattice QCD).

On the theoretical side, potential models have been very successful in describing regular heavy mesons. Using these models, several results were also reported on heavy baryons [3–10]. The spectra of heavy baryons were also studied by other models, such as QCD sum rules [11–14] and heavy quark effective theory [15]. In this aspect, this recent discovery at LHCb provides a good opportunity for testing predictions of these models.

On the other hand, lattice QCD methods provide a unique opportunity to study hadronic physics from first principles, particularly the energy spectra of hadrons. Substantial progress has been made to extract the ground and excited states of charm mesons [16–18]. However, most lattice studies on heavy baryons are confined mainly to the ground states of spin-1/2⁺ and spin-3/2⁺ baryons [19–26]. Following the successful programs in calculating the excited state spectra of light hadrons by the Hadron Spectrum Collaboration (HSC), recently we reported our findings on the excited state spectra of triply charmed baryons [27], doubly charmed baryons [28], and

preliminary results on singly charmed baryons [29–31]. Here we report for the first time our findings on the energy spectra of Ω_c^0 baryons with spin up to 7/2 for both positive and negative parity in detail. By comparing our results with the experimental findings we give a prediction for the quantum numbers of these newly observed subatomic particles.

We use a well-defined procedure that was developed and utilized extensively by HSC in extracting excited states of light mesons [32–34], mesons containing charm quarks [16–18], light and strange baryons [35, 36], as well as charm baryons [27–30]. This method has the following important ingredients:

A. Anisotropic lattice: We use a set of anisotropic gauge field configurations, where dynamics of light and strange quarks are included. The extended time direction and fine temporal lattice spacing (a_t) are very helpful to obtain better resolution of the correlation functions, which is crucial for the reliable extraction of excited states. We use the tree-level Symanzik-improved gauge action along with an anisotropic clover fermion action with tree-level tadpole-improved and three-dimensional stout-link smeared gauge fields. Following are lattice details : size = $16^3 \times 128$; $a_t \sim 0.035$ fm with an anisotropy of 3.5; $m_\pi \sim 391$ MeV; and the number of configurations is 96. Further details of the actions can be found in Refs. [37, 38]. The charm quark mass is tuned by equating the lattice mass of the meson $\eta_c(1S)$ with its physical mass. Details of the charm quark action are given in Ref. [17].

B. Large set of interpolating fields: Hadron spectroscopy on the lattice proceeds through an investigation of the two point correlation functions between the hadron interpolating fields (operators). Because of the octahedral symmetry, interpolating fields on the lattice are not the same as their continuum counterparts, and one needs to construct these interpolating fields according to the reduction of continuum fields into various lattice irreducible representations (irreps), namely, G_1 , G_2 , and H for baryons [39]. Physical states with spins 1/2 and 3/2 can then be obtained only from the G_1 and H irreps respectively, while spin-5/2 states are accessible from both

* Padmanath.Madanagopalan@physik.uni-regensburg.de

† nilmani@theory.tifr.res.in

the H and the G_2 irreps [39]. Following Refs. [35, 40] we construct a large set of baryonic operators which is essential for the reliable extraction of excited states from lattice calculations. These operators transform as irreps of $SU(3)_F$ symmetry for flavor, $SU(4)$ symmetry for Dirac spin of quarks and double cover octahedral group O_h^D of the lattice. The flavor content of $\Omega_c(ssc)$ baryons is similar to that of $\Omega_{cc}(ccs)$ baryons with the role of c and s quark exchanged. Hence, the operator details for Ω_c^0 baryons used in this work follow from Section IIB and Tables II and III of Ref. [28], with the interchange of c and s quarks.

C. Distillation method: We employed a novel technique called “distillation” [41], which is a quark source smearing technique that enables one to compute large correlation matrices (C_{ij}) between a large basis of operators including nonlocal ones, similar to those used in this calculation. Here we implement the method using the lowest 64 eigenvectors of the discretized gauge-covariant Laplacian. The correlation matrices are built from four different source time slices.

D. Variational analysis and spin identification: We utilize a robust analysis procedure, developed by HSC, which is based on the variational study of correlation matrices, C_{ij} . In this method, one solves a generalized eigenvalue problem (GEVP) [42, 43] of the form

$$C_{ij}(t)v_j^n = \lambda_n(t, t_0)C_{ij}(t_0)v_j^n, \quad (1)$$

where $\lambda_n(t, t_0)$ is the n th eigenvalue which is related to the energy of the n th excited state E_n by

$$\lim_{t \rightarrow t_0 \rightarrow \infty} \lambda_n(t, t_0) = e^{-E_n(t-t_0)}. \quad (2)$$

We choose an appropriate reference time slice t_0 in solving GEVP, such that it minimizes a χ^2 -like quantity as defined in Ref. [16]. To associate a spin to an extracted energy level we calculate the overlap factors Z_i^n of an operator O_i defined as $Z_i^n \equiv \langle n | O_i^\dagger | 0 \rangle$ to a state n with energy E_n . These overlap factors carry a memory of the corresponding continuum interpolating field from which O_i was derived and these factors can be obtained from the n th eigenvector v^n of the GEVP. This procedure is being widely used by HSC in all of its spectrum calculations.

Results: Following the above procedures, we are able to extract the energy spectrum of Ω_c^0 baryons with spin up to $7/2$. In Figure 1, we show our results in terms of energy splittings of Ω_c^0 baryons from the mass of the $\eta_c(1S)$ meson. A factor $1/2$ is multiplied with η_c mass to account for the difference in the number of valence charm quarks in the baryon and meson. In general, energy splittings with valence charm content subtracted will have reduced uncertainties originating from the systematics of the charm quark mass parameter in the lattice action and from the ambiguity in the scale setting procedure. Positive and negative parity states are shown on the left- and right-hand sides of the figure, respectively. The vertical height in each box represents 1σ uncertainty, which

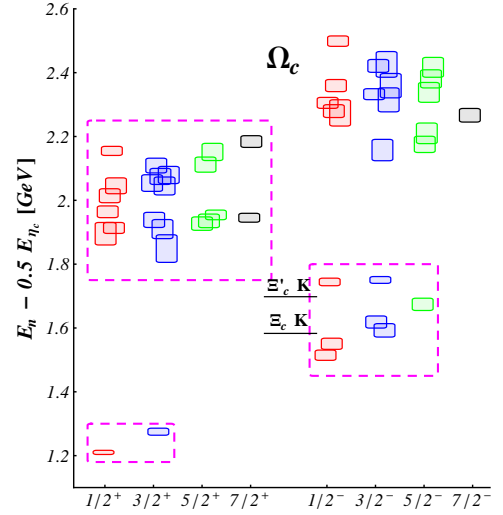


FIG. 1. Spin identified spectra of Ω_c^0 baryons. Here, spectrum is presented in terms of energy splittings of Ω_c^0 baryons from $\eta_c(1S)$ meson. Details of the plot are in the text.

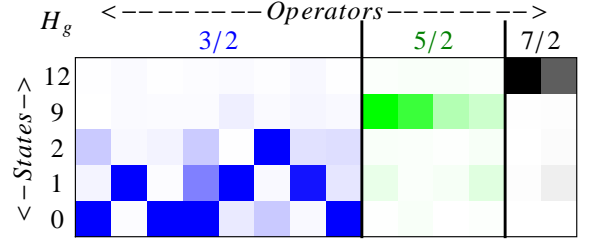


FIG. 2. “Matrix” plot of \tilde{Z} for a few selected operators onto a few spin identified lower energy levels in H_g irrep.

includes statistical and systematic uncertainties from different fit ranges. Throughout this Letter, we follow the color coding for extracted energy levels as follows : spin $1/2$, red; spin $3/2$, blue; spin $5/2$, green; and spin $7/2$ black. The two relevant scattering channels in this calculation are $\Xi_c K$ and $\Xi'_c K$ in s wave. Their lattice values are shown by horizontal black lines and are obtained from Ξ_c , Ξ'_c and K masses calculated on these lattices. The states inside the magenta boxes are those with dominant overlap to operators constructed purely out of the upper two components of the quark spinor. Those are referred to as the nonrelativistic operators. All other operators are relativistic. It is interesting to see that the number of low lying excitations for each spin agrees with the expectations based on the nonrelativistic quark spins which implies a clear signature of $SU(6) \times O(3)$ symmetry in the spectra. A similar $SU(6) \times O(3)$ symmetric nature of the spectra was also observed in light baryons [36] as well as for doubly and triply heavy baryons [27, 28]. It is to be noted that in our variational analysis we have included both nonrelativistic as well as relativistic operators, and still we observe the above symmetry in the low lying spectra.

Next, we briefly describe the procedure followed in as-

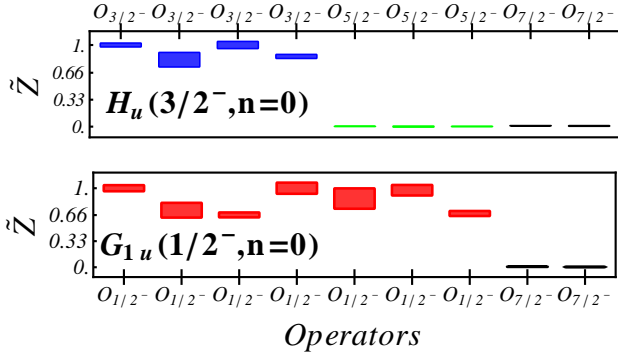


FIG. 3. Histogram plot of \tilde{Z} for the lowest levels in H_u and G_{1u} irreps for a few selected operators.

signing the spin of an extracted energy level leading to the spin identified spectra shown in Figure 1. To explain it, we choose irreps H_g , H_u and G_{1u} (subscripts g and u refer to positive and negative parity, respectively), and show below how a particular energy level that is associated with operators from any of these irreps can be assigned a spin. In Figure 2, we show a representative matrix plot of the normalized overlap factors, $\tilde{Z} = \frac{Z_i^n}{\max[Z_i^n]}$, for a few selected operators on to a few of the lower energy levels in the H_g irrep, where the continuum $3/2^+$, $5/2^+$, and $7/2^+$ states appear. We follow the same color coding as above, while the darkness of the pixel is linearly related to the magnitude of the normalized overlap. From this figure, one can clearly associate the states labeled as 0, 1, and 2 with spin $3/2$, the state 9 with spin $5/2$, and the state 12 with spin $7/2$. In order to further demonstrate the robustness of the procedure, in Figure 3 we present a representative histogram plot of \tilde{Z} values from two different irreps. In the top plot, on the x axis we show various operators in the H_u irrep with their continuum spins and the y axis shows their \tilde{Z} values to a particular energy excitation. This also shows that this energy excitation represents a spin- $3/2^-$ state as it is saturated predominantly from operators that have spin $3/2^-$ in the continuum. In the bottom plot, we show a similar observation in the G_{1u} irrep for an energy excitation that we found to be a spin- $1/2^-$ state. For spin- $5/2$ and $7/2$ states, their \tilde{Z} values need to be compared among different irreps [27, 28, 35, 36]. Spin identifications for all other energy excitations are performed with the same rigor.

With confidence in our procedure for the extraction of energy levels and their spin identification, we finally present our main result. In Figure 4, we show a comparison plot between the extracted lattice energy levels with those from the recently observed Ω_c^0 baryons [2] along with the previously known two other Ω_c^0 baryons [1]. The relevant continuum scattering thresholds are presented on the left-hand side and the noninteracting scattering energies as obtained on these lattices are shown on the right-hand side. It can be seen that our lattice estimate for the hyperfine splitting between spin- $3/2$ and spin-

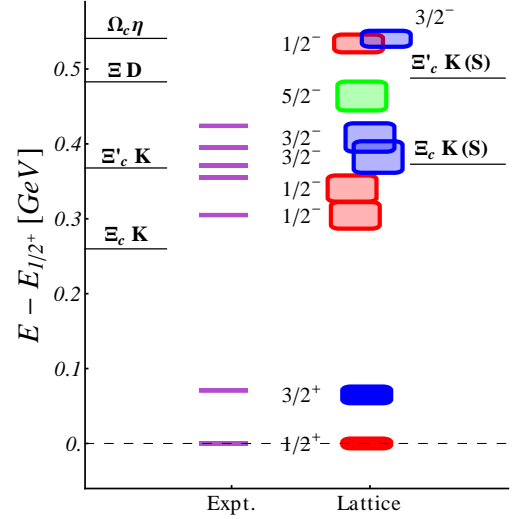


FIG. 4. Comparison plot between experimental and lattice results of Ω_c baryons.

$1/2$ baryons is well in agreement with experiment. The most interesting observation from this comparison is the fact that we observe exactly five energy excitations in the same energy region above the $3/2^+$ state. Two other states are above the scattering levels and thus need to be studied with more rigor. It is also very satisfying to see that among the five new excitations, four are matching with our lattice results. The only remaining excitation, which we assign to be a spin- $5/2^-$ baryon, can possibly be identified to the remaining higher lying experimental candidate. We would like to point out that these results are prediction and not postdiction, as preliminary results of these were already presented at the Charm-2013, 2015 and Lattice-2014 conferences [29–31]. It is to be noted that most other nonlattice calculations [3–15] on Ω_c^0 baryons predicted seven levels in this region. In Table I, we summarize the comparison between experiments and this lattice calculation (called L1), where we denote the i th energy level of Ω_c^0 by $\Omega_c^{0,i}$, while ΔE is the energy difference from the ground state ($\Omega_c^{0,0}$). From the results shown in Figure 4 and Table I, we conclude that the spin-parity quantum numbers of these newly discovered particles are as follows: $\Omega_c(3000)^0$ and $\Omega_c(3050)^0$ have spin-parity $J^P = 1/2^-$, the states $\Omega_c(3066)^0$ and $\Omega_c(3090)^0$ have $J^P = 3/2^-$, while $\Omega_c(3119)^0$ is possibly a $5/2^-$ state. A similar assignment of spin and parity has also recently been made in a potential model calculation [44].

To strengthen our findings, we perform another lattice calculation (called L2) with a totally different set of lattice parameters. We use three dynamical $2+1+1$ flavors HISQ lattice ensembles generated by the MILC Collaboration [45]: $24^3 \times 64$, $32^3 \times 96$, and $48^3 \times 96$ lattices with lattice spacings $\sim 0.12, 0.09$, and 0.06 fm, respectively. For the valence quark propagators, we use overlap action [46]. The details of this lattice set up, charm and

Energy splittings (ΔE)	Experiment		Lattice			
	ΔE	J^P	ΔE (MeV)		J^P	
	(MeV)	[1]	L1	L2		
$E_{\Omega_c^{0,0}} - \frac{1}{2}E_{\eta_c}$	1203(2)	$1/2^+$	1209(7)	1200(10)	$1/2^+$	
$E_{\Omega_c^{0,1}} - E_{\Omega_c^{0,0}}$	70.7(1)	$3/2^+$	65(11)	68(14)	$3/2^+$	
$E_{\Omega_c^{0,2}} - E_{\Omega_c^{0,0}}$	305(1)	?	304(17)	319(19)	$1/2^-$	
$E_{\Omega_c^{0,3}} - E_{\Omega_c^{0,0}}$	355(1)	?	341(18)		$1/2^-$	
$E_{\Omega_c^{0,4}} - E_{\Omega_c^{0,0}}$	371(1)	?	383(21)		$3/2^-$	
$E_{\Omega_c^{0,5}} - E_{\Omega_c^{0,0}}$	395(1)	?	409(19)	403(21)	$3/2^-$	
$E_{\Omega_c^{0,6}} - E_{\Omega_c^{0,0}}$	422(1)	?	464(20)		$5/2^-$	

TABLE I. Comparison of energy splittings of Ω_c^0 baryons between experimental and lattice results. $\Omega_c^{0,i}$ represents the i th energy level.

strange mass tuning are given in Refs. [22, 23]. On these ensembles, we calculate two point correlation functions of Ω_c^0 baryons using conventional local spin-1/2 and 3/2 operators and extract the respective lowest states for both the parities. In Figure 5, we show results from this calculation again as mass splittings from the ground state ($1/2^+$). We also perform continuum extrapolations using $\mathcal{O}(a^2)$ and $\mathcal{O}(a^3)$ forms in lattice spacing, a . The 1σ error bars from $\mathcal{O}(a^3)$ fittings are shown by the shaded regions. In Table I, in the column L2 we show these results which include both statistical as well as all systematic errors. It is quite encouraging to see that lattice results from two completely different setups are consistent with each other, and this ensures again the robustness of the spin assignment procedure utilized in the first calculation. It is to be noted that the results obtained in the L2 calculation rely on conventional single exponential fits of the two point correlation function. Hence, while results for spin-1/2⁺ and -3/2⁺ states are reliable, it is difficult to extract energy levels of states reliably whose energies are close by. In that case, one obtains a single energy level as a mixture of the two. This is indeed what we observed in the L2 results for 1/2⁻ states, which is in the middle of two states obtained in the L1 calculation.

We now discuss the scattering channels relevant to our calculation. For the lowest three states the only possible strong decay channel is $\Xi^+ K^-$, whereas the higher two levels can decay into $\Xi^+ K^-$ and $\Xi'^+ K^-$. Owing to the heavy pion mass ($m_\pi \sim 391$ MeV), scattering levels $\Xi_c^+ K^-$ and $\Xi_c'^+ K^-$ in the s wave, as measured on our lattice, appear at 373 and 488 MeV, respectively, above the ground state, as shown in Figure 4. Both of the extracted spin-1/2⁻ states are below these energy thresholds. On the other hand, spin-3/2⁻ and spin-5/2⁻ states can decay into $\Xi_c^+ K^-$ only via d wave. However, the corresponding noninteracting lattice scattering energies lie significantly above these excitations. Considering the narrow width of the observed resonances [2] and lattice positions of the scattering channels, as discussed above, we believe that the single hadron approximation in our

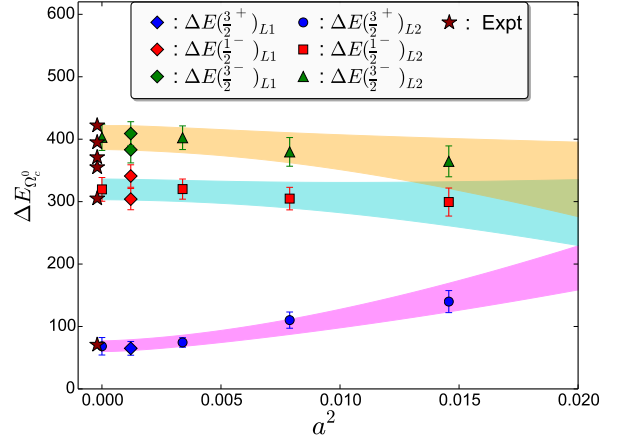


FIG. 5. Mass splittings of the lattice energy levels from the ground state of $1/2^+$ Ω_c^0 baryon, where $\Delta E(J^P) \equiv E(J^P) - E(1/2^+)$. L1 and L2 represent first and second lattice calculations.

calculation, where we have neglected multiparticle operators, will have negligible effects on the energy excitations that we have extracted.

We would also like to point out possible uncertainties in this calculation. The main uncertainties are from the discretization of the heavy charm quark mass. As mentioned previously, we believe that this uncertainty gets reduced by taking appropriate energy differences where the effects of the valence charm quark content is subtracted out. The agreement between lattice and experimental values in the hyperfine splitting between spin-3/2 and spin-1/2 baryons, which is known for its strong discretization artifacts, also justifies the above claim. Furthermore, consistency between our two lattice investigations (L1 and L2) with entirely different systematics confirms that the discretization effects on the mass splittings in the first calculation are indeed under control. The effects from the unphysical light quark mass and small lattice volume are expected to be smaller in Ω_c baryons than those for light baryons, as the former do not have light valence u and d quarks. Our lattice value of the spin-1/2 ground state matches with its experimental value, which further provides confidence to this view. The relative spin ordering of these energy excitations that we assigned here is expected to be unaffected by future lattice calculations with more realistic physical parameters.

Conclusions: In this Letter, we present detailed results from the first nonperturbative calculation on the excited state spectroscopy of Ω_c^0 baryons with spin up to 7/2 and for positive as well as negative parity. Results from this work have direct relevance to the five Ω_c^0 resonances recently discovered by the LHCb Collaboration. We predict the quantum number of these energy excitations as the following: $\Omega_c(3000)^0$ and $\Omega_c(3050)^0$ have spin-parity $J^P = 1/2^-$, the states $\Omega_c(3066)^0$ and $\Omega_c(3090)^0$ have $J^P = 3/2^-$, whereas $\Omega_c(3119)^0$ possibly is a $5/2^-$ state. An elaborate and well-established lattice method is followed for extracting these energy levels and

in identifying their spins. We cross-check these results by performing another lattice calculation with a completely different setup and with better control over systematics. The spin-parity quantum number assigned to these newly observed states is expected to be unaffected by any future lattice calculation with much improved control over the systematic uncertainties.

Acknowledgements: We thank our colleagues within the Hadron Spectrum Collaboration. We are thankful to the MILC Collaboration and, in particular,

to S. Gottlieb for providing us with the HISQ lattices. Computations are carried out on the Blue Gene/P of the ILGTI in TIFR, and on the Gaggles cluster of the Department of Theoretical Physics, TIFR. Chroma [47] and QUDA [48, 49] software are used for this calculation. N. M. would like to thank A. Dighe and P. Junnarkar, and M. P. would like to thank S. Collins for discussions. M. P. also acknowledges support from the Austrian Science Fund FWF: I1313-N27 and the Deutsche Forschungsgemeinschaft under Grant No.SFB/TRR 55.

-
- [1] C. Patrignani *et al.*, Chin. Phys. C **40**, 100001 (2016).
 - [2] R. Aaij *et al.* (LHCb Collaboration), Phys. Rev. Lett. **118**, 182001 (2017).
 - [3] D. Ebert, R. N. Faustov, and V. O. Galkin, Phys. Lett. B **659**, 612 (2008).
 - [4] D. Ebert, R. N. Faustov, and V. O. Galkin, Phys. Rev. D **84**, 014025 (2011).
 - [5] H. Garcilazo, J. Vijande, and A. Valcarce, J. Phys. G **34**, 961 (2007).
 - [6] A. Valcarce, H. Garcilazo, and J. Vijande, Eur. Phys. J. A **37**, 217 (2008).
 - [7] W. Roberts and M. Pervin, Int. J. Mod. Phys. A **23**, 2817 (2008).
 - [8] J. Vijande, A. Valcarce, T. F. Carames, and H. Garcilazo, Int. J. Mod. Phys. E **22**, 1330011 (2013).
 - [9] T. Yoshida, E. Hiyama, A. Hosaka, M. Oka, and K. Sadato, Phys. Rev. D **92**, 114029 (2015).
 - [10] Z. Shah, K. Thakkar, A. K. Rai, and P. C. Vinodkumar, Chin. Phys. C **40**, 123102 (2016).
 - [11] E. Bagan, M. Chabab, H. G. Dosch, and S. Narison, Phys. Lett. B **287**, 176 (1992).
 - [12] C. S. Huang, A. I. Zhang, and S. L. Zhu, Phys. Lett. B **492**, 288 (2000).
 - [13] Z. G. Wang, Phys. Lett. B **685**, 59 (2010).
 - [14] H. X. Chen *et al.*, Phys. Rev. D **91**, 054034 (2015).
 - [15] G. Chiladze and A. F. Falk, Phys. Rev. D **56**, R6738 (1997).
 - [16] J. J. Dudek, R. G. Edwards, N. Mathur, and D. G. Richards, Phys. Rev. D **77**, 034501 (2008).
 - [17] L. Liu *et al.* [Hadron Spectrum Collaboration], JHEP **1207**, 126 (2012).
 - [18] G. Moir, M. Peardon, S. M. Ryan, C. E. Thomas, and L. Liu, JHEP **1305**, 021 (2013).
 - [19] N. Mathur, R. Lewis, and R. M. Woloshyn, Phys. Rev. D **66**, 014502 (2002).
 - [20] R. Lewis, N. Mathur, and R. M. Woloshyn, Phys. Rev. D **64**, 094509 (2001).
 - [21] S. Durr, G. Koutsou, and T. Lippert, Phys. Rev. D **86**, 114514 (2012).
 - [22] S. Basak, S. Datta, M. Padmanath, P. Majumdar, and N. Mathur, PoS LATTICE **2012**, 141 (2012), arXiv:1211.6277.
 - [23] S. Basak, S. Datta, A. T. Lytle, M. Padmanath, P. Majumdar, and N. Mathur, PoS LATTICE **2013**, 243 (2014), arXiv:1312.3050.
 - [24] Y. Namekawa *et al.* [PACS-CS Collaboration], Phys. Rev. D **87**, 094512 (2013).
 - [25] Z. S. Brown, W. Detmold, S. Meinel, and K. Orginos, Phys. Rev. D **90**, 094507 (2014).
 - [26] P. Perez-Rubio, S. Collins, and G. S. Bali, Phys. Rev. D **92**, 034504 (2015).
 - [27] M. Padmanath, R. G. Edwards, N. Mathur, and M. Peardon, Phys. Rev. D **90**, 074504 (2014).
 - [28] M. Padmanath, R. G. Edwards, N. Mathur, and M. Peardon, Phys. Rev. D **91**, 094502 (2015).
 - [29] M. Padmanath, R. G. Edwards, N. Mathur, and M. Peardon, arXiv:1311.4806.
 - [30] M. Padmanath, R. G. Edwards, N. Mathur, and M. J. Peardon, PoS LATTICE **2014**, 084 (2015), arXiv:1410.8791.
 - [31] M. Padmanath and N. Mathur, arXiv:1508.07168.
 - [32] J. J. Dudek, R. G. Edwards, M. J. Peardon, D. G. Richards, and C. E. Thomas, Phys. Rev. D **82**, 034508 (2010).
 - [33] J. J. Dudek, R. G. Edwards, M. J. Peardon, D. G. Richards, and C. E. Thomas, Phys. Rev. Lett. **103**, 262001 (2009).
 - [34] J. J. Dudek, R. G. Edwards, M. J. Peardon, D. G. Richards, and C. E. Thomas, Phys. Rev. D **83**, 071504 (2011).
 - [35] R. G. Edwards, J. J. Dudek, D. G. Richards, and S. J. Wallace, Phys. Rev. D **84**, 074508 (2011).
 - [36] R. G. Edwards, N. Mathur, D. G. Richards, and S. J. Wallace, [Hadron Spectrum Collaboration], Phys. Rev. D **87**, 054506 (2013).
 - [37] R. G. Edwards, B. Joo, and H. -W. Lin, Phys. Rev. D **78**, 054501 (2008).
 - [38] H. -W. Lin *et al.* (Hadron Spectrum Collaboration), Phys. Rev. D **79**, 034502 (2009).
 - [39] R. C. Johnson, Phys. Lett. B **114**, 147 (1982).
 - [40] S. Basak *et al.* (Lattice Hadron Physics (LHPC) Collaboration), Phys. Rev. D **72**, 074501 (2005).
 - [41] M. Peardon *et al.*, (Hadron Spectrum Collaboration), Phys. Rev. D **80**, 054506 (2009).
 - [42] C. Michael, Nucl. Phys. B **259**, 58 (1985).
 - [43] M. Luscher and U. Wolff, Nucl. Phys. B **339**, 222 (1990).
 - [44] M. Karliner and J. L. Rosner, Phys. Rev. D **95**, 114012 (2017).
 - [45] A. Bazavov *et al.* (MILC Collaboration), Phys. Rev. D **87**, 054505 (2013).
 - [46] H. Neuberger, Phys. Lett. B **417**, 141 (1998).
 - [47] R. G. Edwards *et al.* (SciDAC and LHPC and UKQCD Collaborations), Nucl. Phys. Proc. Suppl. **140**, 832 (2005).
 - [48] M. A. Clark, R. Babich, K. Barros, R. C. Brower, and C. Rebbi, Comput. Phys. Commun. **181**, 1517 (2010).
 - [49] R. Babich, M. A. Clark, and B. Joo, arXiv:1011.0024.